Acta of Bioengineering and Biomechanics
Vol. 18, No. 4, 2016

Original paper
DOI: 10.5277/ABB-00642-2016-02

Biomechanical evaluation of a novel Limb Prosthesis Osseointegrated Fixation System designed to combine the advantages of interference-fit and threaded solutions

PIOTR PROCHOR*, SZCZEPAN PISZCZATOWSKI, EUGENIUSZ SAJEWICZ

Department of Biocybernetics and Biomedical Engineering, Faculty of Mechanical Engineering,
Białystok University of Technology, Białystok, Poland.

Purpose: The study was aimed at biomechanical evaluation of a novel Limb Prosthesis Osseointegrated Fixation System (LPOFS) designed to combine the advantages of interference-fit and threaded solutions. *Methods:* Three cases, the LPOFS (designed), the OPRA (threaded) and the ITAP (interference-fit) implants were studied. Von-Mises stresses in bone patterns and maximal values generated while axial loading on an implant placed in bone and the force reaction values in contact elements while extracting an implant were analysed. Primary and fully osteointegrated connections were considered. *Results:* The results obtained for primary connection indicate more effective anchoring of the OPRA, however the LPOFS provides more appropriate stress distribution (lower stress-shielding, no overloading) in bone. In the case of fully osteointegrated connection the LPOFSs kept the most favourable stress distribution in cortical bone which is the most important long-term feature of the implant usage and bone remodelling. Moreover, in fully bound connection its anchoring elements resist extracting attempts more than the ITAP and the OPRA. *Conclusions:* The results obtained allow us to conclude that in the case of features under study the LPOFS is a more functional solution to direct skeletal attachment of limb prosthesis than the referential implants during short and long-term use.

Key words: *finite element analysis, direct skeletal attachment, implants*

1. Introduction

Nowadays, the most widely used method of attaching external prosthesis to a lower limb stump is to use a prosthetic socket with appropriate mechanisms attached, for instance, frame locks, which makes it possible to attach the prosthesis connectors with a socket [4], [6], [13], [20]. It is most commonly performed on the basis of measurements taken from the amputee's cast which allows for creating a negative and ultimately a positive to accurately reflect the state of the limb after amputation [6]. Originally made socket requires a quick exchange due to the stump's tendency to change the volume after the surgery. This process is caused by a bad circulation of body fluids and postoperative edema, which stabilise during the healing period [4], [6], [13], [20].

Due to the continuous work, the geometry of the stump can be changed under the influence of various loads acting on it. For this reason, it is advisable to supervise the prosthetic socket every three years and take the appropriate adjustments or replacing it if required. Improperly fitting connection may result in, among others, irritation and abrasion of the skin (in case of too tight connection) or sliding the funnel from the stump (if coupled less tightly) [4], [6], [13], [20].

* Corresponding author: Piotr Prochor, Department of Materials and Biomedical Engineering, Białystok University of Technology, ul. Wiejska 45a, 15-351 Białystok, Poland. Tel: 502575276, e-mail: piotrekprochor@gmail.com
Received: January 12th, 2016
Accepted for publication: March 20th, 2016

The processes and related activities mentioned prove a necessity of developing new stump-external prosthesis connection techniques. One such solution may be known, but rarely used implanting system, which examples can be the OPRA (Osseointegrated Prostheses for the Rehabilitation of Amputees) and the ITAP (Intraosseous Transcutaneous Amputation Prosthesis) [15]. Implanting systems as the prosthesis suspensions are the development of the dental implant concept [4], [13], [15], [24].

Implanting system is a single-element (the ITAP) or multi-element (the OPRA), also known as modular, solution and is permanently implanted in bone during surgery after reaming marrow cavity [4], [6], [13], [16], [20]. In order to anchor the implant more effectively, interference-fit connections are used (with irregular shapes and splines increasing interaction with surrounding bone), as in the case of the ITAP solutions or a suitable thread used in the OPRA. Each of these connections has its advantages and disadvantages. In the case of an interference-fit invaluable advantage is the reduction of the stresses in the radial direction of bone (that cause its cutting), which are very high in the case of the threaded connection [13]. However, excessive bone stress that arises at the bone–implant contact causes the local resorption [11], [21], [22], which after some time results in loosening of the implant connected to bone with an interference-fit. This phenomenon also occurs in the case of a threaded connection [13] even though it is firmly anchored in bone by the thread teeth which provide a larger implant–bone contact area.

Apart from the risk factors mentioned above, the use of the implantation system may cause infections around the implant [4], [8], [20]. However, it also provides invaluable advantages [10], [18], [23], often impossible to obtain while using the prosthetic socket. The advantages include: user's comfort, quick fastening, no skin abrasions, no need of constant putting in and removing the prosthesis connecting element and others [4], [6], [16], [18], [20], [23]. A properly designed implanting system can provide new, yet unexplored advantages of fixing prostheses, and therefore a growing interest in this method is visible.

The purpose of the present paper is to introduce a new design of an implant for direct skeletal attachment of limb prosthesis that ensures a better stress distribution in bone (than the implants of the reference) while preserving anchoring elements. These properties have been confirmed by finite element analyses presented in the following sections.

2. Materials and methods

2.1. The design of the new type of implant for direct skeletal attachment of limb prosthesis

Structure

The Limb Prosthesis Osteointegrated Fixation System (LPOFS) consists of two parts: the glass-particle-reinforced PEEK (Polyether Ether Ketone) fixture screwed in bone and the abutment placed in the fixture (Fig. 1). The fixture is hollow and consists of: a blocking cap, a cylindrically shaped segment A, and a triple-notched segment B of a conical shape with the spiral teeth on the outer part which increase in height with distance from the cap (the outer diameter of the teeth ϕ_1 is equal to the diameter of the outer segment A – it prevents rubbing the teeth against bone tissue during implantation of the fixture). Inside the segment A there is a metric thread for attaching the abutment and outside a properly scaled thread for cortical bone type HA [19]. Additionally, in order to provide better osteointegration Ti-coating is used on the fixture's external surface.

The abutment (made of Ti6Al4V) consists of: the head (description of the exact shape of the head is omitted, as it can be freely selected according to the needs of the connection with the exoprosthesis), the head's shaft, the blocking cap, the cylindrical segment C notched outside with the metric thread and the conical segment D that ends with the closure cap whose diameter (ϕ_2) is equal to the inner diameter of the cylindrical segment A of the fixture. A porous layer (e.g., Ti-coating) is applied to the head's shaft in order to allow the soft tissue (skin) to ingrow the surface of the implant, which will reduce the risk of potential infection.

The efficiency of the materials considered was confirmed by Tomaszewski's implant project [21]. However, it differs significantly from the design described in terms of less beneficial way of implantation. The individual elements of the LPOFS are presented in Fig. 1.

The method of implantation process

The first step is reaming the marrow cavity for the length of the fixture and a diameter slighly smaller than the outer diameter of the fixture's segment A (the diameter of the bottom of the thread's notches). The next step is pushing the fixture into the drill hole until the start of the thread and finishing the implantation by screwing in the implant. It is followed by placing the abutment inside the fixture and pushing it in to the

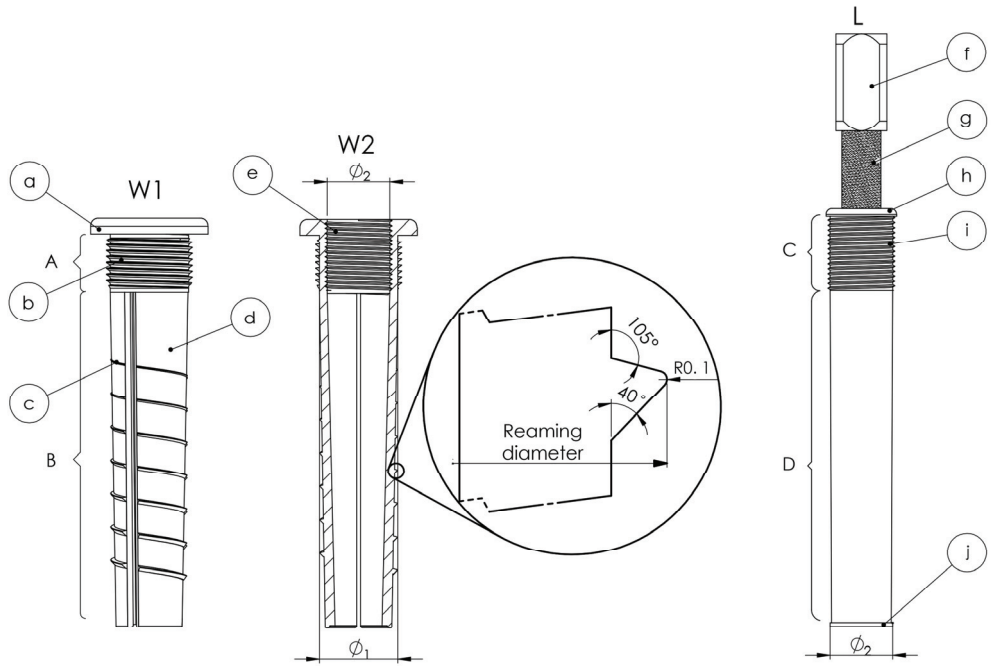

Fig. 1. The LPOFSs structure: W1 – the fixture (view): (A) cylindrical segment A; (B) conical, triple notched segment B; (a) blocking cap; (b) the implant thread for cortical bone; (c) helically cut teeth with an outer diameter equal to the outer diameter (ϕ_1) of segment A (bottom of the thread's notches); (d) Ti-coating; W2 – the fixture (cross-section): (e) metric thread for attaching the abutment; L – abutment (view): (C) cylindrical segment C; (D) conical segment D; (f) head; (g) head's shaft with a porous layer; (h) abutment's blocking cap; (i) metric thread for fixture attachment; (j) closure cap

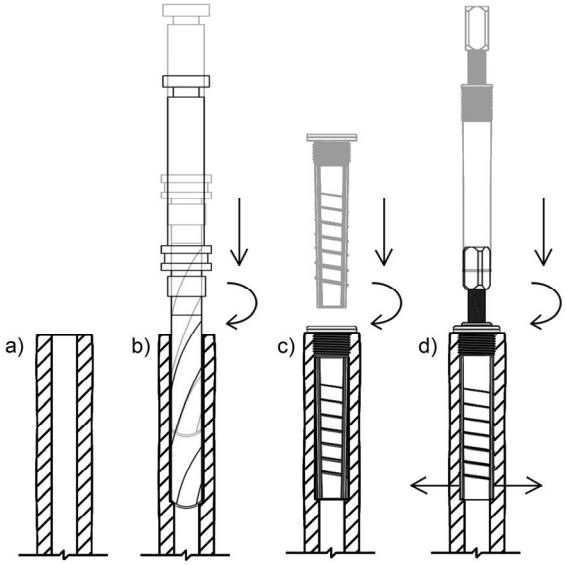

Fig. 2. The method of implantation: (a) long bone after amputation; (b) reaming the marrow cavity; (c) pressing and then screwing the fixture in bone; (d) pressing and then screwing the abutment in until it shuts the closure cap – thrusting the teeth into cortical bone tissue

beginning of the thread. The final step is to screw the abutment in until it shuts the closure cap of the abutment at the end of the fixture. A schematic way of implantation process is presented in Fig. 2.

Pressing the abutment in the fixture screwed in bone causes expansion of B segments and thrusting its teeth into cortical bone. The aim is to preserve the benefits of the threaded and interference-fit connections.

2.2. Three dimensional CAD and FE models

2.2.1. CAD models of implants and cortical bone

The LPOFS solid model, the models of two implants of the reference: the OPRA (threaded) and the ITAP (interference-fit), and model of cortical bone were made in SolidWorks2015 software (Fig. 3).

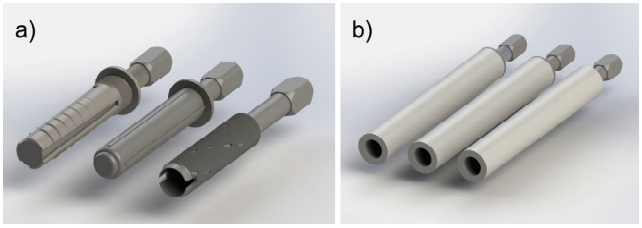

Fig. 3. (a) CAD models of the LPOFS and the implants of the reference (from left: the LPOFS, the ITAP, the OPRA); (b) their positioning in cortical bone – made in SolidWorks2015

Table. 1. The overall dimensions of the CAD models

Parameter	LPOFS	OPRA	ITAP
Length of cortical bone implanted section [mm]	100	100	100
Outer diameter of cortical bone implanted section (Designed implant, ITAP) / Diameter of the top of the thread's notches (OPRA) [mm]	20	20	20

Parameter	Cortical bone
Outer diameter [mm]	30
Marrow cavity diameter [mm]	18
Length [mm]	200

In order to get comparable results, modelling included implants' overall dimensions and identical cortical bone dimensions. Each implantation system includes the same, simplified head's shape of an implant, to which an external prosthesis is attached. In the case of the ITAP system the healing cap was omitted, as it does not affect the load transfer and serves only for ingrowth of the skin. Overall dimensions of the models are summarised in Table 1.

2.2.2. FE models based on CAD designs

Previously created CAD models were exported to ANSYS Workbench 16.2. Materials used for analyses and their properties are shown in Table 2.

To consider bone orthotropic properties a cylindrical coordinate system was used. Discretisation of models was performed using tetrahedral, 10-node finite elements Solid187 [1]. Face and edge sizing was performed in the spots where cortical bone remained adjacent to the implant's surface. This allowed more accurate results to be obtained in regions where the expected stresses in cortical bone were supposed to be the greatest. Due to implants' symmetry it was possible to divide the models into two symmetrical parts (using symmetry region operation) and analyse one of them. These changes resulted in decreasing the total number of elements in the mesh which lead to hastening the calculation process. Contact elements (Conta174 and Targe170) were also applied to include reciprocal interaction between the bone and the implant [1]. The parameters of FE models are included in Table 3.

The differences in the quantity of nodes and elements are the result of the implants' constructions. For this reason, the ITAP of the simpliest construction has the lowest quantity, while the OPRA the highest due to the thread noched on the whole length of its fixture.

Table 2. The mechanical properties of cortical bone and Ti6Al4V

Part name	Material model	Young's modulus [GPa]			Poisson's ratio	Shear modulus [GPa]	Density [kg/m^3]	Ref.
LPOFS	Isotropic (Glass-particle-reinforced PEEK)	12.5			0.400	4.46	1320	[21]
OPRA	Isotropic (Ti6Al4V)	110.0			0.330	41.35	4500	[5], 17]
ITAP								
Cortical bone	Orthotropic	Direction	x (radial)	12.0	0.376	4.53	1910	[2], [9]
			y (transverse)	13.4	0.222	5.61		
			z (longitudinal)	20.0	0.235	6.23		

Table 3. Number of nodes in finite element net and number of elements in finite element mesh for different implant models

Model of implant placed in bone	Quantity of nodes	Quantity of 10-node tetrahedral elements	Quantity of contact elements
LPOFS	175066	100659	10349
OPRA	194537	108447	17479
ITAP	136578	78647	14879

2.2.3. Boundary conditions and loadings

To determine the implant–bone connection effectiveness the following cases were analysed:

Case 1 – primary connection between bone and the implant:
- Variant 1a – axial loading on the implant's head;
- Variant 1b – extracting the implant from bone.

Case 2 – fully osteointegrated connection between bone and the implant:
- Variant 2a – axial loading on the implant's head;
- Variant 2b – extracting the implant from bone.

Case 1 – the primary connection between bone and the implant. It is characterised by the absence of osteointergration resulting in friction between the surfaces of the implant and bone. In this case mutual sliding between the contact elements of adjacing surfaces was allowed. The friction coefficient between bone and the implant was set to 0.4 [22]. The calculations were conducted using a Gauss point detection method and augmented Lagrange formulation.

$$p = \frac{\delta_r \tau}{\frac{R}{E_b}\left(\frac{r_b^2 + R^2}{r_b^2 - R^2} + \nu_b\right) + \frac{R}{E_i}(1 - \nu_i)} \tag{1}$$

where

p – implant–bone pressure in the interference-fit connection [MPa];

δ_r – radial intererence between the implant and reaimed marrow cavity [mm];

τ – interference-fit connection area of contact;

R – nominal radius of connection [mm];

E_i – Young's modulus of the implant material [MPa];

E_b – Young's modulus of bone in radial direction [MPa];

r_b – external radius of bone [mm];

ν_i – Poisson's ratio of the implant material;

ν_b – Poisson's ratio of bone in radial direction.

Due to the space between the B segment's notches of the LPOFS the interference-fit connection area of contact (τ) is descreased by 22.17% comparing to ITAP-bone connection, effectively lowering the pressure (Table 4).

Case 2 – fully osteointegrated connection between bone and the implant. To illustrate the assumed conditions, the implant–bone connection was set as fully bound which also resulted in binding the contact elements to prevent their mutual sliding. The bone adjustment to the implant in the post-implantation period, resulting in significant lowering of pressure in interference-fit connection was also taken into account. Consequently, the pressure described in Table 4 was omitted in the analysis.

Table. 4. Pressure of interference-fit connections and used calculation values

Model	δ_r [mm]	R [mm]	E_i [GPa]	E_b [GPa]	r_b [mm]	ν_i	ν_b	τ [%]	**P [MPa]**
LPOFS	0.1	10	12.5	12	15	0.400	0.376	77.83	**26.62**
ITAP			110			0.330		100	**40.00**

Analysing interference-fit connections (in the cases of the ITAP and the LPOFS) required determining the primary influence of the implant on bone tissue (Fig. 4). To achieve this, the pressure during the post-operative period of the implant–bone connection was set as an additional boundary condition on bone adjacent, external surfaces of the implants. The respective pressure values were estimated using formula (1) adapted from [3].

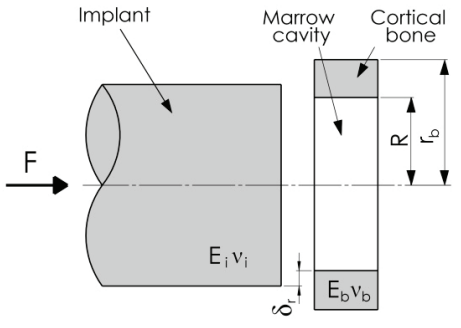

Fig. 4. Implant–bone interference-fit parameters

The fixed support was established at the distal surface of cortical bone in case 1 as well as in case 2 (Fig. 5).

Two variants of loadings were considered in both cases. In "variants a" axial force was applied on the head of each (Fig. 5a) to evaluate the implant's displacement and stress pattern in bone. The hip joint carries the load 2 to 4 times greater than the weight of the body during gait [7], [12]. Based on the data presented the force affecting the head of the implant was estimated from 2000 N to 4000 N. The assumptions correspond to a human of a weight of 50 to 100 kg. In order to obtain ref-

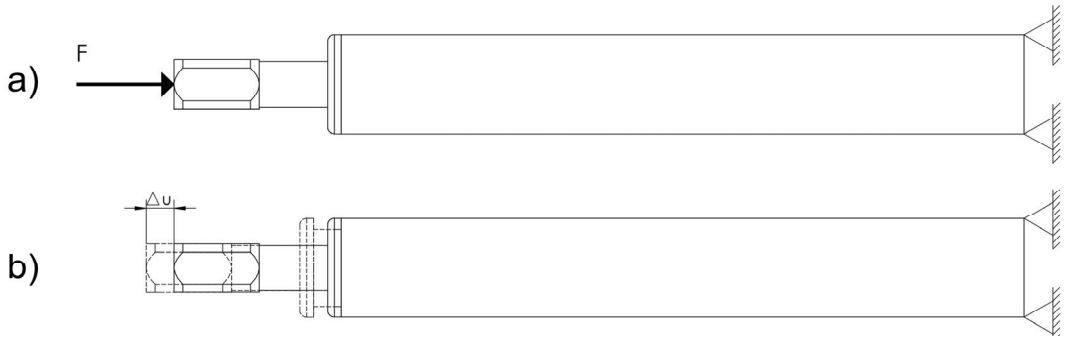

Fig. 5. Fixed support, force and displacement locations a) variants a; b) variants b

erential data, a stress pattern in loaded non-implanted bone was also considered.

In "variants b" the values of force reaction (longitudinal direction) in contact elements on implant –bone interface were obtained while extracting the implant from the bone. The purpose of the test was to evaluate the efficiency of anchoring elements on the basis of the obtained force values. To simulate the extraction process, a model was created in which the implant was extracted from bone, while applying the displacement value from 0 mm to 0.1 mm (Fig. 5b).

3. Results

3.1. Determining the primary stability

The obtained results of maximal values of von-Mises stresses in bone, implants axial displacements during implant loading as well as force reaction (longitudinal direction) in contact elements during implant extraction are presented in Table 5.

Table 5. Maximal values of von-Mises stresses in bone, implant axial displacement (bone loading) and force reaction in contact elements (implant extraction) – primary stabilisation

Variant 1a	Max. values of von-Mises stress in bone [MPa]				Implant axial displacement [mm]		
Force F [N]	LPOFS	ITAP	OPRA	Non-implanted	LPOFS	ITAP	OPRA
2000	9.80	15.60	4.70	4.42	0.027	0.035	0.026
2500	11.79	18.28	5.97	5.52	0.035	0.042	0.032
3000	15.38	20.96	7.27	6.63	0.042	0.048	0.039
3500	19.54	23.65	8.58	7.74	0.050	0.054	0.045
4000	24.07	26.33	9.90	8.84	0.057	0.061	0.052

Variant 1b	Max. values of force reaction (longitudinal direction) in contact elements on implant-bone interface [N]		
Implant displacement Δd [mm]	LPOFS	ITAP	OPRA
0.02	578.75	559.55	564.88
0.04	1049.50	646.50	1131.30
0.06	1518.70	769.84	1698.00
0.08	1986.00	775.78	2265.00
0.10	2451.70	778.81	2832.20

The stress patterns for the least favourable variant (F = 4000 N) and comparison of obtained force reaction values in contact elements during implant extraction (Δd = 0.02 up to 0.1 mm) are shown in Fig. 6 and Fig. 7.

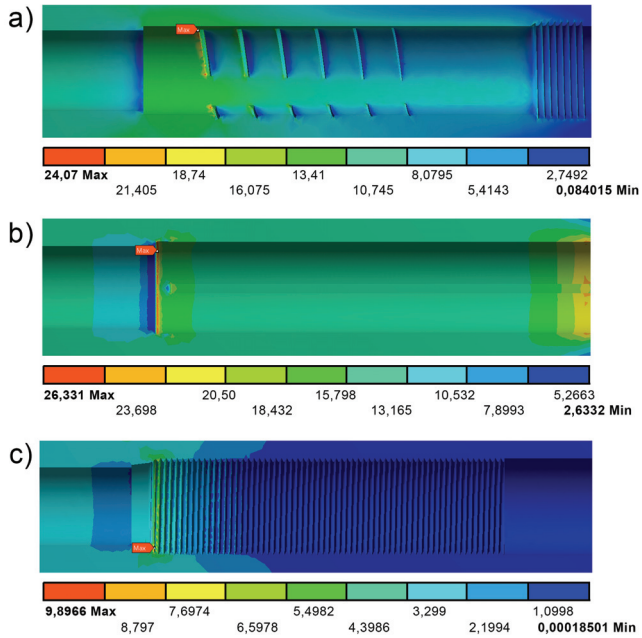

Fig. 6. The stress patterns in bone [MPa] (primary stabilisation) upon axial loading of the implant's head with a force of 4000 N: (a) LPOFS; (b) ITAP; (c) OPRA

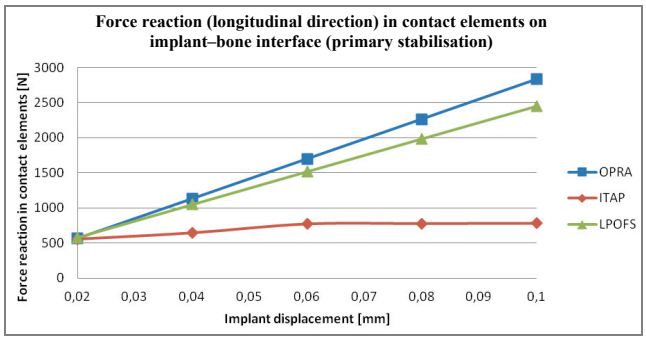

Fig. 7. The force reaction (longitudinal direction) in contact elements on implant–bone interface [N] (primary stabilisation) while displacing the implant by 0.02 up to 0.1 mm

To increase the precision of analyses of the stresses in bone upon axial loading on the implant's head, the stress patterns for the path set 12 mm away from bone's axis were studied (Fig. 8). Comparing these patterns with the results obtained for intact bone allow one to evaluate stress-shielding.

The results obtained are presented in Fig. 9.

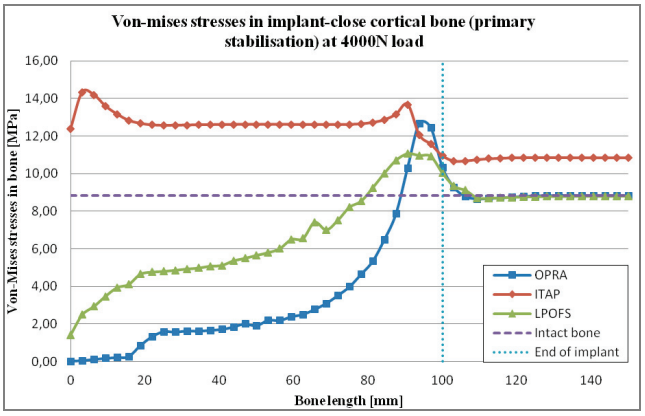

Fig. 9. Von-Mises stresses in an implant-close cortical bone (primary stabilisation) at 4000 N load

3.2. Fully osteointegrated connection analysis

The results for fully osteointegrated connections are presented in Table 6.

Just like in the primary stabilisation case, optimal stress distribution and the presence of anchoring elements in fully osteointegrated connection are equally important. For this reason stress patterns, implant displacement and force reactions were analysed for the same loading conditions (considering two variants "a" and "b") as in the primary stabilisation's case (Figs. 10, 11).

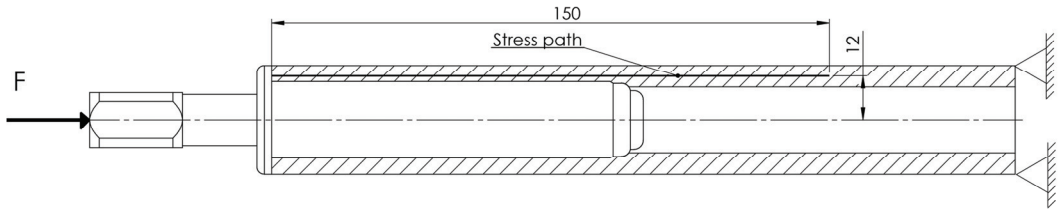

Fig. 8. Stress path length and location

Table 6. Maximal values of von-Mises stresses in bone, implant axial displacement (bone loading) and force reaction in contact elements (implant extraction) – fully osteointegrated connection

Variant 2a	Max. values of von-Mises stress in bone [MPa]				Implant axial displacement [mm]		
Force F [N]	LPOFS	ITAP	OPRA	Non-implanted	LPOFS	ITAP	OPRA
2000	12.74	40.24	11.31	4.42	0.023	0.024	0.022
2500	15.92	50.30	14.14	5.52	0.028	0.030	0.028
3000	19.11	60.36	16.97	6.63	0.034	0.036	0.033
3500	22.29	70.42	19.80	7.74	0.040	0.042	0.039
4000	25.48	80.47	22.63	8.84	0.045	0.048	0.044

Variant 2b	Max. values of force reaction (longitudinal direction) in contact elements on implant-bone interface [N]		
Implant displacement Δd [mm]	LPOFS	ITAP	OPRA
0.02	699.93	600.39	606.85
0.04	1399.86	1200.80	1213.70
0.06	2099.79	1801.20	1820.60
0.08	2799.72	2401.60	2427.40
0.10	3499.65	3002.60	3034.30

Following the method presented in Figure 8, the stresses patterns in implant-close cortical bone was determined, as shown in Figure 12.

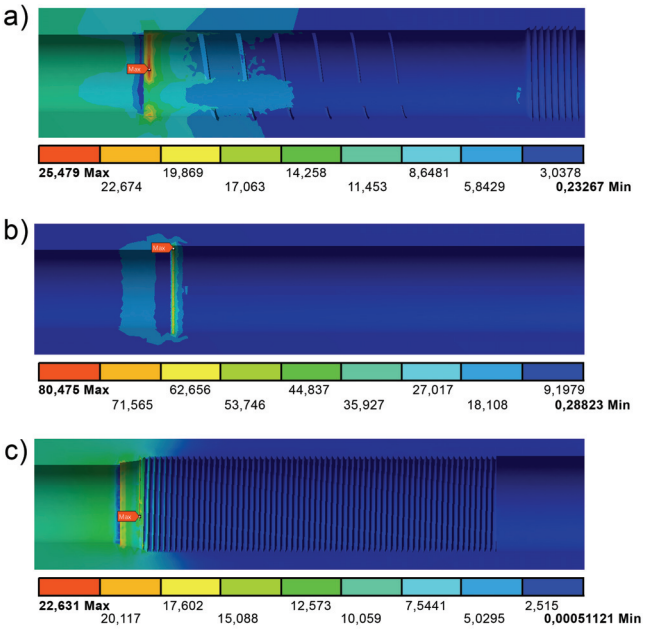

Fig. 10. The stress patterns in bone [MPa] (fully osteointegrated connection) upon axial loading of the implant's head with a force of 4000 N: (a) LPOFS; (b) ITAP; (c) OPRA

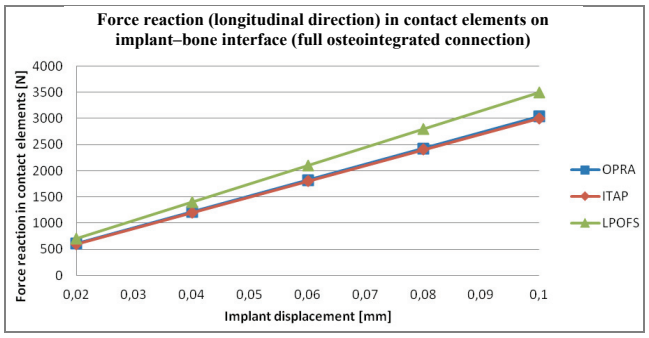

Fig. 11. The stress patterns in bone [MPa] (fully osteointegrated connection) while displacing the implant by 0.02 up to 0.1 mm: (a) LPOFS; (b) ITAP; (c) OPRA

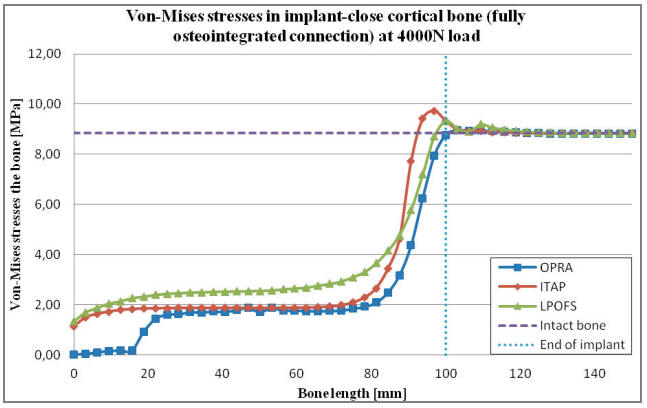

Fig. 12. Von-Mises stresses in implant-close cortical bone (fully osteointegrated connection) at 4000N load

4. Discussion

The paper presents the design of the Limb Prosthesis Osseointegrated Fixation System (LPOFS) and compares it with two reference implants: the ITAP and the OPRA [15].

The A segment's notched thread and the B segment's spiral teeth are among the LPOFS's features that increase the primary and secondary stability of the implant. Along with the length of the fixture, the teeth increase in height, allowing for better anchoring of the implant at the point where the highest stresses occur in farther bone–implant contact area. The implant penetrates soft tissues after implantation. For this reason, a porous layer is applied onto the shaft's head of the abutment to enable skin–implant integration.

The influence of implants' geometry on stress patterns in cortical bone, as well as the effectiveness of anchoring elements in the primary and fully osteointegrated connection cases were observed in the analyses presented. Based on the results, the biomechanical evaluation of the LPOFS in comparison with the implants of the reference (the OPRA and the ITAP) was conducted.

In terms of the stress concentration (in the case of primary connection) while axial loading of the implant with a force of 4000 N (the least favourable case) the ITAP ranks last. The stresses of high values, reaching 26.33 MPa, are visible in the distal part of the implant –bone connection. These values exceed approximately 3 times the stresses in a loaded, non-implanted bone. A similar concentration of stresses is visible in the OPRA system, however their maximal values are significantly lower, reaching 9.90 MPa. Meanwhile the concentration of stresses in the LPOFS's case occurs near the highest (the most distal) spiral tooth of the fixture, reaching a peak value of 24.07 MPa, placing it in between the reference implants. Additionaly, the stress paths indicate that in terms of stress distribution the most effective is the one with the LPOFS (Fig. 9). The curves prove that the initial (implanted) part of bone (0–100 mm) carries higher loads than in the OPRA implant (lower stress-shielding). This suggests the presence of the proper initiating bone-remodeling impulse, lowering bone's mechanical damage vulnerability. In the case of the ITAP's stress pattern a large overloading is noticeable at the whole length of the analysed section of bone (12.38 MPa up to 14.33 MPa, considering 0–100 mm segment). The lack of anchoring elements results in transferring the load by the implant's blocking cap only. Increased stress value (10.85 MPa) in relation to the other cases (around 8.84 MPa for: the LPOFS, the OPRA, intact bone) that appears over 100 mm is caused by the interference-fit pressure. For this reason, bone is exposed to overloading that may exceed the natural loads even by 19%. Therefore, the stress distribution for the ITAP is worse than the stress distribution for the designed LPOFS. Despite the interference-fit pressure of the LPOFS, bone is not overloaded beyond 0–100 mm section. It is a consequence of the multi-element construction, where the fixture screwed in bone is made of the low Young's modulus material (PEEK – 12.5 GPa). Implants' microdisplacement values while axial loading are similar in each case reaching 57 μm on averge. The obtained values of force reaction (longitudinal direction) in contact elements, while extracting the implant from cortical bone (implant displacement by 0.02 up to 0.1 mm), allow the effectiveness of anchoring elements to be estimated. In the case of primary connection the OPRA had the most effective anchoring elements, while the LPOFS's anchoring elements were worse by around 13.4%. The ITAP's anchoring effectiveness was the least favourable (worse than the OPRA's by 73.5%) which was caused by the lack of thread or teeth that are cut into bone tissue after implantation and that are opposing extraction attempts.

In the analysis of fully osteointegrated connection, the concentration of stresses while axially loading the implant were slightly different for the LPOFS (25.48 MPa), and the OPRA (22.63 MPa) cases. The ITAP's case notes the most significant change increasing from 26.33 MPa to 80.47 MPa. The concentrations were situated in the distal segment bone–implant connection. Similarly to the primary connection, the implant displacement (in fully osteointegrated connection) upon axial loading slightly differs in each case, but its average value decreased to 46 μm. The most beneficial stress distribution in bone (the lowest stress-shielding) occurs while loading the LPOFS. During that process the stress values transferred by the initial section of bone (0 mm–80 mm) are estimated to be 26% higher than in the reference implant, providing a more beneficial initiating bone remodeling impulse. The effectiveness of combining interference-fit and threaded connection features in the LPOFS proves itself during implant extraction in fully osteointegrated connection. The obtained values of force reaction (longitudinal direction) in contact elements allow us to conclude that in terms of analysing features the LPOFS is characterised by the most favourable anchoring elements. Received force reaction values are around 15.3% higher than in the cases of extracting implants of reference. It means that the LPOFS's anchoring

elements put more resistance to extracting attempts than the ITAP's and the OPRA's.

The results were obtained using the idealised model of cortical bone. The purpose was to determine the effectiveness of the bone–implant connection without the influence of bone's geometry. In real conditions, the anchoring elements' position in relation to the anatomical curves of the bone will affect the stress patterns. If it changes, so will the stress patterns. For this reason, in the next stages of the LPOFS's studies, the most optimal in-bone position should be optimised to obtain its maximal functionality after implantation.

Both solutions, the ITAP and the OPRA, have been applied in practice [15], therefore, it can be stated that the structure developed will function properly in in-vivo conditions. Because of the unique features, the implant developed by the authors has been submitted as an invention to Polish Patent Office (application no. P.416266) [14].

5. Conclusions

The biomechanical evaluation confirms the effectiveness of the Limb Prosthesis Osseointegrated Fixation System designed by the authors. It allows us to conclude that the designed implant will be potentially a more functional solution in comparison with the reference ones presented.

Acknowledgement

This research was performed as a part of projects MB/WM/17/2016 and S/WM/1/2014, and financed with the use of funds for science of Ministry for Science and Higher Education.

References

[1] Ansys, Inc., Ansys Mechanical APDL Element Reference, Release 15.0, 2013.

[2] ASHMAN R.B., COWIN S.C., VAN BUSKIRK W.C., RICE J.C., *A continuous wave technique for the measurement of the elastic properties of cortical bone*, J. Biomech, 1984, 17(5), 349–361, DOI: 10.1016/0021-9290(84)90029-0.

[3] BOZKAYA D., MÜFTÜ S., *Mechanics of tapered interface fit in dental implants*, J. Biomech., 2003, 36(11), 1649–58.

[4] BRÅNEMARK R., BERLIN O., HAGBERG K., BERGH P., GUNTERBERG B., RYDEVIK B., *A novel osseointegrated percutaneous prosthetic system for the treatment of patients with transfemoral amputation: A prospective study of 51 patients*, Bone Joint J., 2014, 96-B(1), DOI: 10.1302/0301-620X.96B1.31905.

[5] CAPITANU L., FLORESCU V., BADITA L.L., *New concept in durability improvement of hip total joint endoprostheses*, Acta Bioeng. Biomech., 2014, 16(1), 75-82, DOI: 10.5277/abb140110.

[6] COLLINS D., KARMARKAR A., RELICH R., PASQUINA P., COOPER R., *Review of research on prosthetic devices for lower extremity*, CRC Rev. Biomed. Eng., 2006, 34(5), 379–439.

[7] GODEST A.C., BEAUGONIN M., HAUG E., TAYLOR M., GREGSON P.J., *Simulation of a knee joint replacement during a gait cycle using explicit finite element analysis*, J. Biomech., 2002, 35(2), 267–275.

[8] HELGASON B., PÁLSSON H., RÚNARSSON T.P., FROSSARD L., VICECONTI M., *Risk of failure during gait for direct skeletal attachment of a femoral prosthesis: a finite element study*, Med. Eng. Phys., 2009, 31(5), 595–600. DOI: 10.1016/j.medengphy.2008.11.015.

[9] LI Y., YANG C., ZHAO H., QU S., LI X., *New Developments of Ti-Based Alloys for Biomedical Applications*, Materials, 2014, 7(3), 1709–1800, DOI: 10.3390/ma7031709.

[10] LUNDBERG M., HAGBERG K., BULLINGTON J., *My prosthesis as a part of me: A qualitative analysis of living with an osseointegrated prosthetic limb*, Prosthet. Orthot. Int., 2011, 35(2), 2007–2214.

[11] MOONEY V., PREDECKI P.K., RENNING J., GRAY J., *Skeletal extension of limb prosthesic attachment – problems in tissue reaction*, J. Biomed. Mater Res., 1971, 5(6), 143–159.

[12] MORRISON J.B., *The mechanics of the knee joint in relation to normal walking*, J. Biomech., 1970, 3(1), 51–61.

[13] NEBERGALL A., BRAGDON C., ANTONELLIS A., KÄRRHOLM J., BRÅNEMARK R., MALCHAU H., *Stable fixation of an osseointegated implant system for above-the-knee amputees: titel RSA and radiographic evaluation of migration and bone remodeling in 55 cases*, Acta Orthop., 2012, 83(2), DOI: 10.3109/17453674.2012.678799.

[14] Patent application: Two-element implant for direct skeletal attachment of limb prosthesis, application number: P.416266.

[15] PITKIN M.C., *Design features of implants for direct skeletal attachment of limb prostheses*, J. Biomed. Mater Res. A, 2013, 101(11), 3339–3348.

[16] PITKIN M.C., CASSIDY R., MUPPAVARAPU J., RAYMOND M., SHEVTSOV O., GALIBIN S.D., *New method of fixation of in-bone implanted prosthesis*, J. Rehabil. Res. Dev., 2013, 50(5), 709–722.

[17] POCHRZĄST M., BASIAGA M., MARCINIAK J., KACZMAREK M., *Biomechanical analysis of limited-contact plate used for osteosynthesis*, Acta Bioeng. Biomech., 2014, 16(1), 99–105, DOI: 10.5277/abb140112.

[18] ROCHMINSKI R., SIBNSKI M., SYNDER M., *Osseointegration as a method of direct stabilization of amputation prostheses to the bone*, Chir. Narzadów Ruchu Ortop. Pol., 2011, 76(1), 36–40.

[19] Standard ISO 5835:1991 – Implants for surgery – Metal bone screws with hexagonal drive connection, spherical undersurface of head, asymmetrical thread – Dimensions.

[20] TILLANDER J., HAGBERG K., HAGBERG L., BRÅNEMARK R., *Osseointegrated titanium implants for limb prosthesis attachments – infectious complications*, Clin. Orthop. Relat. R, 2010, 468(10), DOI: 10.1007/s11999-010-1370-0.

[21] TOMASZEWSKI P.K., VAN DIEST M., BULSTRA S.K., VERDONSCHOT N., VERKERKE G.J., *Numerical analysis of an osseointegrated prosthesis fixation with reduced bone failure*

risk and peroprosthetic bone loss, J. Biomech., 2012, 45(11), 1875–1880.

[22] TOMASZEWSKI P.K., VERDONSCHOT N., BULSTRA S.K., VERKERKE G.J., *A comparative finite-element analysis of bone failure and load transfer of osseointegrated prostheses fixations*, Ann. Biomed. Eng., 2010, 38(7), 2418–2427.

[23] WEBSTER J.B., CHOU T., KENLY M., ENGLISH M., ROBERTS T.L., BLOEBAUM R.D., *Perceptions and acceptance of osseointegration among individuals with lower limb amputations: A prospective survey study*, J. Prosthet. Orthot., 2009, 21(4), 215.

[24] ZHENG L., YANG J., HU X., LUO J., *Three dimensional finite element analysis of a novel osteointegrated dental implant designed to reduce stress peak of cortical bone*, Acta Bioeng. Biomech., 2014, 16(3), 21–28, DOI: 10.5277/abb140303.